Chem. Educator **2000,** *5,* 8–13

A Metallic Surface Corrosion Study in Aqueous NaCl Solutions Using Atomic Force Microscopy (AFM)

Andrew M. Skolnik,[†] W. Christopher Hughes,[‡] and Brian H. Augustine[†,*]

James Madison University, Harrisonburg, VA 22807, augustbh@jmu.edu

Abstract: We report an upper-division undergraduate solid-state materials chemistry experiment involving the pit and crevice corrosion of a copper surface caused by an aqueous NaCl solution simulating a seawater environment. Surface corrosion of the copper can be shown quite dramatically using atomic force microscopy (AFM) within only hours of exposure to the saline solution. The copper surfaces can also be treated with an alkanethiol solution to form a self-assembled monolayer (SAM) on the surface. When exposed to the salt-water solution, the SAM layer is shown by AFM to protect the surface from corrosion. We have also shown that several different AFM analysis methods are needed to adequately quantify the surface features including roughness and power spectral density. This experiment enables students to not only see how AFM can be used to observe changes in surface morphology, but also learn to develop an understanding of the analysis techniques used to quantify AFM data.

Introduction

Since the development of the atomic force microscope in the mid-1980s [1], atomic force microscopy (AFM) has been a technique used to characterize the surface morphology of many different materials with near atomic resolution [2]. As AFM is becoming more widely available in the undergraduate university setting, there is a need to develop laboratory demonstrations and experiments for undergraduate students in the application of AFM to the study of surfaces in materials chemistry and physics. We have chosen to demonstrate some of the capabilities of AFM by examining the real-world problem of metal corrosion in salt water. The topic of surface corrosion is both important technologically and the subject of current materials science research [3]. This experiment can be readily implemented to dramatically show the capabilities of AFM, and it clearly illustrates some potential difficulties in quantification of AFM data. This laboratory also demonstrates a practical application of self-assembled monolayers (SAM) to surfaces and their ability to protect a metallic surface from corrosion.

Implementation of this experiment requires only polished copper sheet and easily prepared alkanethiol and NaCl solutions. Contact mode AFM is used to both qualitatively and quantitatively characterize the metal surfaces. We have chosen copper surfaces because the time frame required to observe corrosion is fast enough that changes can be seen in the course of one laboratory period (3 h), commercially available alkanethiol reagents self-assemble to copper, and copper sheet is inexpensive.

Theoretical Background

Atomic Force Microscopy. Atomic force microscopy is a surface analytical tool developed during the mid-1980s by Binnig, Quate and Gerber [1] as a daughter technique to scanning tunneling microscopy (STM) [4]. These and other recently developed imaging techniques can be broadly categorized as scanning probe microscopy (SPM) techniques [5]. The term scanning probe refers to a probe that is scanned in a raster pattern across a surface and is capable of responding to small perturbations to the probe. The nature of the surface–probe interaction determines the type of microscopy being performed. In the case of STM, an electrically conductive and atomically sharp metal probe (typically Pt/Ir wire) is brought within nanometers of a conducting or semiconducting surface. When a bias is applied between the surface and the probe, electrons can quantum mechanically tunnel into available electron states in either the probe or the surface depending on the direction of the bias. Because the tunneling current is exponentially dependent on the surface-to-probe distance, nearly all of the tunneling current is produced from the lowermost atoms in the probe. For this reason, STM is able to achieve true atomic resolution. Researchers have realized atomic images in real space such as the work popularized by Eigler and colleagues at IBM Almaden [6].

Atomic force microscopy uses a cantilever probe with a tip that has been microfabricated using standard semiconductor manufacturing techniques such as photolithography and etching. Typically, these cantilevers are made from either amorphous Si_3N_4 or crystalline Si. In the case of AFM, the surface–probe interactions are intermolecular van der Waals forces. The probe is fabricated such that the radius of curvature is typically 20–60 nm. As the probe is brought into close proximity to the surface, it responds to attractive or repulsive van der Waals forces at nanometer distances. AFM can be operated either in direct contact with the surface, known as contact mode, or at the resonance frequency of the cantilever, known as intermittent contact or Tapping Mode. This experiment was performed in contact mode because it is both simplest to understand and the most readily available AFM technique at the undergraduate university level. In order to detect such small forces (typically nN), the cantilever must be fabricated so that the spring constant of the probe is lower

[*] Address correspondence to this author. Email:augustbh@jmu.edu
[†] Department of Chemistry MSC 7701
[‡] Department of Physics MSC 7702

© 2000 Springer-Verlag New York, Inc., S1430-4171(00)01350-9, 10.1007/s00897990350a, 510008ba.pdf

than that of the intermolecular forces between the atoms on the surface to avoid damage to the surface being imaged, yet have a high enough resonance frequency so as not to be susceptible to vibrational instabilities. These probes have been commercially fabricated for a decade with typical force constants ranging from 0.06 N m^{-1} for Si_3N_4 up to 100 N m^{-1} for Si probes.

In order to detect deflections of the cantilever from the interacting van der Waals forces, an optical detection scheme has been developed. Light from a laser diode is reflected off of the backside of the cantilever onto a position-sensitive photodetector (PSPD) array. The array consists of either two detectors placed one on top of the other, or four detectors with two on the top and two on the bottom. As the probe is scanned across the surface, small deflections in the cantilever are magnified in an optical lever effect. An analogy of this effect can be readily demonstrated by holding a laser pointer in one's hand and directing it onto a wall or screen. Small movements of the hand result in large movements of the laser spot, and this effect is amplified as one moves the distance of the laser pointer source further from the screen. The measured signal from the PSPD is simply the voltage difference between the top and bottom detectors, which changes as the cantilever is deflected up or down relative to the center position.

The final requirement of scanning probe microscopy is a feedback mechanism. This is needed to prevent the probe from crashing into large features on a surface. The typical feedback mechanism employed in contact mode AFM is called the *constant deflection* method. In this case, the cantilever is repositioned at each data point to maintain a constant cantilever deflection which is determined by a set-point voltage. The set-point voltage is derived from the signal from the PSPD. In reality, the cantilever is not continually scanning across the surface, but is stepped to each data point, the deflection is measured, the cantilever is repositioned to maintain a constant force on the surface, and the process continues until a three-dimensional image is digitally generated with information recorded in lateral position (x and y) and height (z) at each pixel. AFM is capable of a lateral resolution of approximately 1 nm and a vertical resolution of 0.1 nm. The reason that true atomic imaging is not possible with AFM is because the van der Waals forces extend over several nanometers compared to tunneling currents which decrease exponentially on the angstrom-length scale. The maximum scan size is dependent on the piezoelectric scanner used and may be different with each instrument. Other scanning probe interactions include friction force microscopy, magnetic force microscopy, scanning capacitance microscopy, and scanning thermal microscopy, among others.

Corrosion of Metal. The pit and crevice corrosion mechanism is described in most undergraduate materials science textbooks [7]. Corrosion of a metal surface (M) in an aqueous NaCl solution proceeds by the following mechanism:

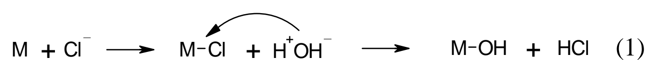

A chloride ion first chemisorbs to the metal surface (M). This surface is then quickly hydrolyzed by water to form an insoluble metal hydroxide. The metal hydroxide formation is what accounts for the pits and the crevices that appear on the surface of the metal. Corrosion becomes apparent to the naked eye as a polished and reflective surface will no longer specularly reflect, but will scatter the incident light. In the case of metallic copper, copper hydroxide, which appears as an insoluble blue precipitate over time, is formed.

The concentration of the salt solution in this study was chosen to simulate oceanographic conditions. The average salinity of ocean water is reported to be approximately 34.5 practical salinity units (PSU) based on an ocean salinity map produced by the National Oceanographic and Atmospheric Administration [8]. A PSU is equivalent to grams per liter; thus, the average salinity corresponds to a 0.58 M NaCl solution. This concentration was used to demonstrate that corrosion is a real and viable problem for metal structures in or near seawater environments.

Self-Assembled Monolayer Surfaces. During the last decade, there has been much work on controlling the properties of surfaces through the use of organic molecular monolayer thin films. The most widely used system has been the self-assembly of alkanethiolate adsorbates onto gold surfaces [9]. Alkanethiols spontaneously form a dense molecular monolayer at room temperature with several transition metal surfaces including gold, silver, and copper through a strong thiolate bond to the metal surface [10]. There have been many research articles published on this rapidly developing field, and the reader is referred to reviews by Xia and Whitesides [10] or to an *MRS Bulletin* cover story [11]. One of the intriguing features of these SAM surfaces is the ability to carefully control the surface chemistry of a metal. One can vary the surface free energy from extremely hydrophobic, for a methyl terminated alkane chain, to extremely hydrophilic, for an alcohol or carboxylic acid terminated alkane chain.

It has also been reported by several groups that thin films or surface monolayer coatings on a metal can help prevent surface corrosion [12–17]. Thin-film corrosion protection is clearly a technologically and economically important consideration. In this experiment, an alkanethiol solution was used to produce a dense, ordered SAM on the copper surface. Past studies have shown that an alkanethiol SAM has protected copper from air exposure for up to 300 days [16].

Quantitative Analysis of AFM Data. One of the primary reasons that AFM is a particularly powerful microscopy technique is that the data is digitally stored and can readily be treated mathematically to quantitatively determine the characteristics of a surface [18–20]. Furthermore, one can compare two different surfaces quantitatively rather than qualitatively in a straightforward fashion. Complex mathematical tools such as Fourier or fractal analysis can be routinely performed on commercially available software supplied with the AFM instrument. The simplest and most common method used for the observation of changes in surface topography is called the root mean square (RMS) roughness calculation (R_q). This roughness calculation is based on finding a median surface level for the image and then evaluating the standard deviation within the image. The equation for determining the surface roughness is [20]

$$R_q = \sqrt{\frac{1}{N^2}\sum_{i=1}^{N}\sum_{j=1}^{N}\left(H(i,j)-\bar{H}\right)^2}$$

© 2000 Springer-Verlag New York, Inc., S1430-4171(00)01350-9, 10.1007/s00897990350a, 510008ba.pdf

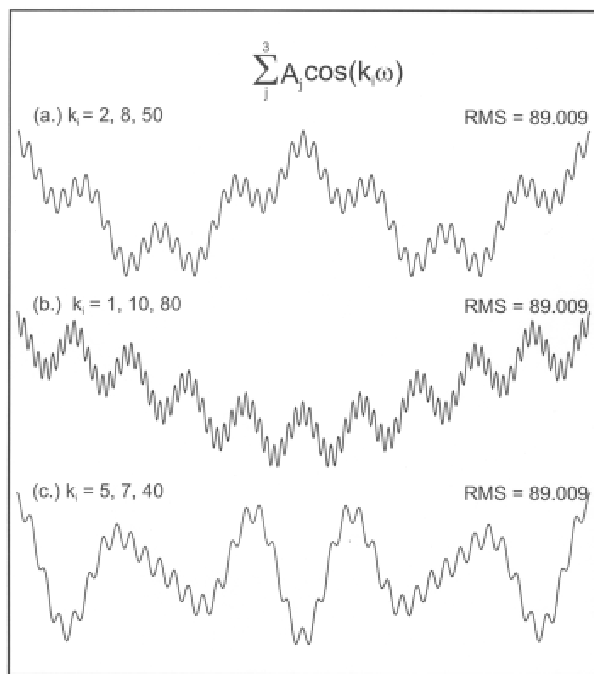

Figure 1. Calculated superposition of cosine functions, each having identical RMS roughness values, using three different frequency components, k_i, indicated above each curve. The amplitudes, *A*, for each are 100, 50, and 25. (Adapted from ref 21.)

where *i* and *j* are the pixel locations on the AFM image, *H* is the average value of the height across the entire image, and *N* is the number of data points in the image (AFM images are typically stored as 256 × 256 or 512 × 512 data arrays). The primary limitation of this algorithm is that it does not show the lateral spacing of various surface features. In other words, the roughness calculated for surfaces with different spatial features may be identical even though optical and atomic force microscopy would suggest that there is a difference in roughness [20–22]. Figure 1 illustrates this as first reported by Spanos and Irene [21]. Three calculated cosine functions with different frequencies and amplitudes yield identical RMS roughness values even though these three surfaces would be very different to a materials scientist due to the difference in spatial frequency of the surface features.

Power spectral density (PSD) is a technique that calculates power (roughness amplitude squared) as a function of spatial wavelengths of the features that are contributing to the surface image [23]. PSD utilizes a Fourier decomposition of an image into spatial frequencies. A complete mathematical treatment of this is beyond the scope of this paper, but the reader is referred to Fang, et al. [23] and Kitching, et al. [22] and references therein for a more complete description of the PSD calculation. When comparing two PSD calculations, the *x* axis is a function of the spatial wavelength and the *y* axis is intensity on a logarithmic scale. With this technique it is possible to see what size features contribute most to an image. For example, if one has a perfectly regular grating repeating in the *x* direction, the PSD will yield one peak at the wavelength of the grating pitch. Smaller features have a higher frequency and thus will appear more intensely in a rougher surface than in a smoother surface.

Experimental

Copper Sample Preparation. Flat copper sheet (McMaster-Carr) was cleaned for 5 min each in acetone, isopropyl alcohol, and deionized water using an ultrasonic cleaner. In between each ultrasonic clean, the copper was dried using compressed nitrogen. Copper was then polished using a high-speed rotary polisher such as a Dremel tool and polishing compound until the copper surface appeared reflective. The copper was then cut into approximately 1-by-1-cm squares. We have found that the type of copper sheet purchased is extremely important. Much of the commercially available copper stock is actually copper alloyed with beryllium. Be is alloyed with Cu to both strengthen the material (alloy hardening) and to inhibit corrosion—a desirable property in most machining applications, but not for this experiment. The corrosion resistance of Cu–Be alloys makes this experiment impractical for one laboratory period.

A saturated (<1 mM) alkanethiol solution was prepared by dissolving hexadecanethiol (Aldrich) in fresh absolute ethanol (Aaper). This solution was then placed into a Petri dish. Copper pieces were immersed in the alkanethiol solution for 24 h and the Petri dish was covered to form a self-assembled monolayer (SAM) on the Cu surface as determined by estimating the contact angle [24] of a drop of deionized water to be $>100^\circ$ on the surface. All glassware should be thoroughly washed and dried before using the alkanethiol solution and all preparations should be performed in a hood. After treatment with alkanethiol, the copper samples were washed with ethanol and dried with compressed nitrogen. The SAM treated copper pieces will henceforth be referred to as *protected copper*.

An unprotected piece of copper was placed along with freshly protected samples in a 0.58 M NaCl solution for 2.5 h at room temperature. These samples were then taken out of solution, dried with compressed nitrogen, and imaged with the AFM. We also prepared SAM-protected samples two weeks earlier in the manner previously described and stored them in air. These were then placed in the NaCl solution to observe whether an older SAM surface would be able to effectively protect the copper surface from corrosion.

All atomic force microscopy images were obtained on a Digital Instruments Nanoscope III Multimode AFM operating in contact mode in air. The lateral scan size was 25 µm at a scan rate of 1.3 Hz and a set point of 0.0 V. Standard silicon nitride contact-mode cantilevers were used with a force constant of ~0.12 N m^{-1}. Samples were mounted on magnetic pucks using double-sided tape. All of the AFM images reported in this paper have identical *x*, *y*, and *z* scales so that a direct comparison may be made between images.

Optical microscopy images were generated by recording the information from a digital CCD camera (Digital Instruments Optical Viewing System) onto VHS tape from the NTSC output of the video screen using a digital frame grabbing card (MicroVIDEO DC30 Plus) and software (Microsoft VidCap). The scale was calibrated by capturing an optical image of a microfabricated calibration grating supplied by Digital Instruments that has a regular periodic structure with a 20.00 µm peak to peak pitch.

Laboratory Implementation. We have used this laboratory in an upper-division materials characterization course (Mats 381) and feel that the experiment is appropriate for relatively small sections (under 15) of junior- and senior-level laboratories such as one would encounter in a physical chemistry or an advanced inorganic chemistry course. If there is more than one AFM available, this experiment could readily be performed in parallel. For our study, students were divided into four groups of two and signed up for three-hour blocks of time using the AFM instrument. The students had been lectured on the principles of AFM prior to the laboratory section. Each group began the experiment by polishing and cleaning the Cu samples the day before the AFM study, and the SAM-protected samples were immersed in the alkanethiol solution 24 h prior to the AFM study. Both the NaCl and alkanethiol solutions were prepared at the beginning of the week of the experiment.

© 2000 Springer-Verlag New York, Inc., S1430-4171(00)01350-9, 10.1007/s00897990350a, 510008ba.pdf

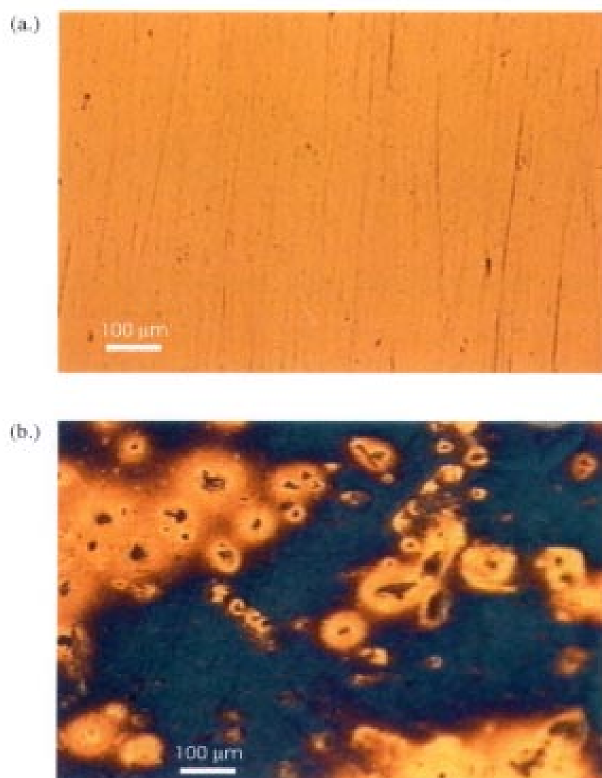

Figure 2. Optical micrographs of (a) as-polished copper surface and (b) unprotected copper surface after 2.5-h exposure to 0.58 M NaCl solution. 100 µm bar is indicated in lower left-hand corner.

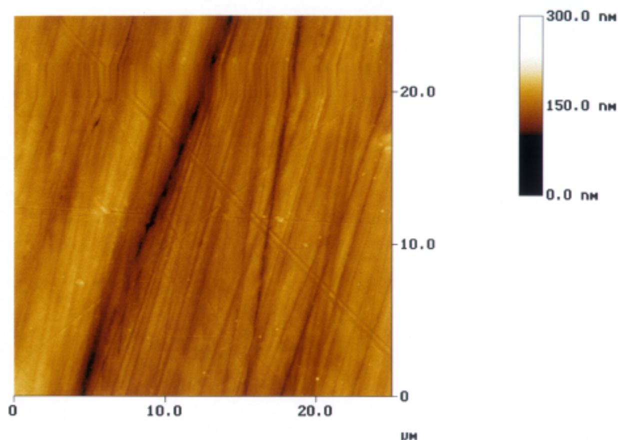

Figure 3. Atomic force microscopy image of as-polished copper surface.

At the start of the experiment, one as-polished Cu sample was immersed in the NaCl solution, and the SAM-protected Cu sample was placed in a second beaker with the NaCl solution. These were allowed to react for approximately 2 hours. While these were reacting, an as-polished sample was mounted on the AFM, the laser was aligned to the cantilever, and the as-polished sample was imaged. During the imaging, details of the AFM data acquisition and analysis software were discussed with the students. After data acquisition, the students calculated the roughness and power spectral density using the Digital Instruments data analysis software. The unprotected and the SAM-protected samples were then removed from the NaCl solution, rinsed, imaged, and analyzed after a 2-h exposure.

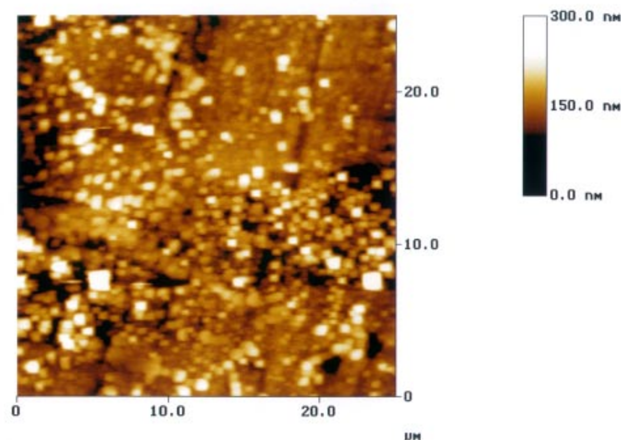

Figure 4. Atomic force microscopy image of unprotected copper surface after 2.5-h exposure to 0.58 M NaCl solution.

Results and Discussion

Immediately upon removing the samples from the solutions it was apparent that corrosion had occurred on the unprotected copper as it was no longer reflective and had a bluish appearance, whereas the SAM-protected copper was still specular. The two-week-protected sample was also reflective after the 2.5-h exposure to the salt water solution. Optical microscopy of the unprotected copper surface shows this striking blue hue indicating surface corrosion shown in Figure 2(b) compared to as-polished copper shown in Figure 2(a). The vertical streaks in the as-polished sample are due to scratches from the polishing process. One does not observe the blue color on either of the SAM-protected surfaces in optical microscopy after exposure to the salt solution, and the surfaces qualitatively appear very similar to the control sample shown in Figure 2(a).

AFM of the as-polished copper control surface is shown in Figure 3. Again, the vertical features are due to polishing damage. This could be improved experimentally by metal-lographic lapping or other more sophisticated sample preparation techniques. We have chosen the rotary polisher, however, because it is simple for undergraduate students to learn how to use without prior microscopy sample preparation experience, and it allows for rapid sample preparation. The unprotected copper surface shown in Figure 4 indicates the presence of square features prevalent throughout the surface ranging from approximately 600 nm to 1.5 µm. These features are typical of corrosion features seen in Cu, which has a face centered cubic crystal lattice. Corrosion typically occurs along the crystal faces of the face-centered-cubic lattice. The interested reader is referred to a recent review of STM corrosion studies of copper by Magnussen and Behm [25]. The freshly SAM-protected copper surface is shown in Figure 5, and the two-week-old SAM-protected copper is shown in Figure 6. The former appears quite similar to the control (Figure 3), and the latter is beginning to exhibit some signs of the square formations but not nearly the same extent as the unprotected sample in Figure 4.

As previously mentioned, it is important to do this experiment with pure copper sheet. We also repeated this experiment using *half-hard* copper sheet, which is a Cu–Be alloy. We found that samples immersed in the NaCl solution

© 2000 Springer-Verlag New York, Inc., S1430-4171(00)01350-9, 10.1007/s00897990350a, 510008ba.pdf

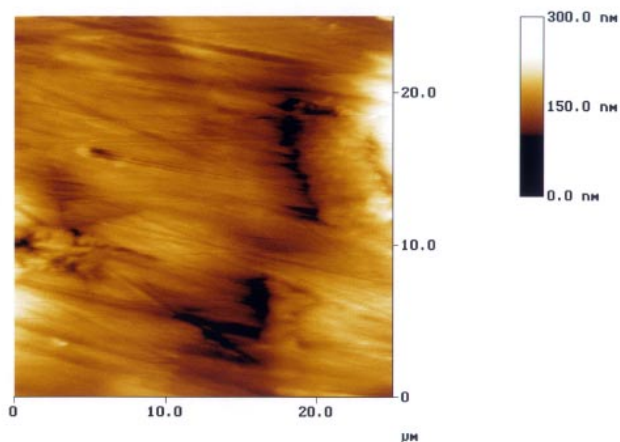

Figure 5. Atomic force microscopy image of SAM-protected copper surface. Surface was exposed to a saturated (<1 mM) hexadecanethiol solution for 24 h prior to 2.5-h exposure in 0.58 M NaCl solution.

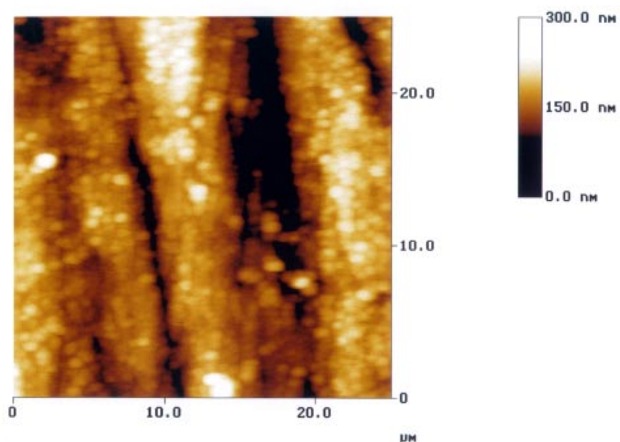

Figure 6. Atomic force microscopy image of two-week-old SAM-protected copper surface. Surface was exposed to a saturated (<1 mM) hexadecanethiol solution for 24 h, then stored in air for two weeks. This sample was then exposed to 0.58 M NaCl solution for 2.5 h and imaged.

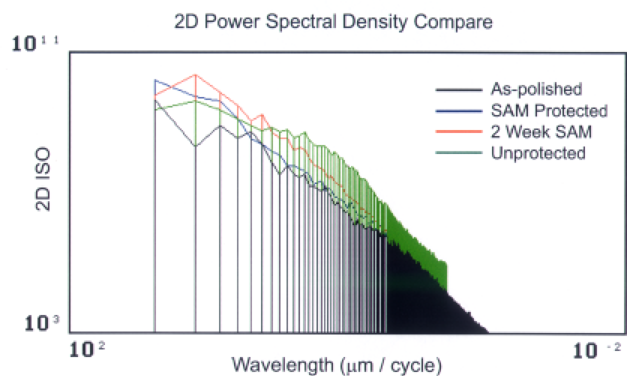

Figure 7. Two-dimensional power spectral density (2-D PSD) comparison of as-polished (shown in black), SAM-protected (shown in blue), two-week-protected (shown in red), and unprotected (shown in green).

Table 1. AFM Data

Sample	RMS (*Rq*) Roughness (nm)	Power (nm^2)
As-polished copper (control)	13.434	0.831
Unprotected copper	32.991	14.7
Fresh SAM-protected copper	23.040	0.974
Two-week SAM-protected copper	33.918	2.3

without protection took several weeks to exhibit a commensurate degree of corrosion. This is because half-hard copper is alloyed to both harden and inhibit corrosion in machined parts. This has lead to an interesting discussion with students about corrosion resistance in alloys, and methods of corrosion prevention in materials such as stainless steel.

Before quantifying the AFM data, all images were flattened using a first-order flatten routine provided in the Digital Instruments analysis software. A RMS roughness measurement was then calculated on each sample and reported in Table 1. The RMS roughness data suggests that the two-week-old SAM-protected copper has a greater surface roughness than the unprotected copper even though the AFM images (Figures 4 and 6, respectively) clearly appear to show that the unprotected copper surface is rougher. This dilemma indicates that either our perception of roughness is not correct, or the RMS roughness is not an adequate quantitative measure of these surfaces. This apparent dilemma is solved with the use of a power spectral density analysis of the copper surfaces.

Following the RMS roughness measurements, a two-dimensional power spectral density (2-D PSD) calculation was performed on the images and plotted against each other as shown in Figure 7. Recall that the PSD shows the contribution to an image of different frequency features. In other words, peaks to the left side of the *x* axis in Figure 7 are long-wavelength (low-frequency) features, and peaks to the right side of the *x* axis are short wavelength (high-frequency) features. What this means is that the low-frequency polishing scratches seen in Figures 3, 5, and 6 will have a larger contribution relative to the smaller (600 nm to 1.5 µm) features exhibited by the unprotected sample. The smaller features will appear as high-frequency peaks, and this is exactly what is observed in Figure 7. At low frequencies the polishing scratches in the as-polished (shown in black), the SAM-protected (shown in blue), and the two-week sample (shown in red) are strongest, while the unprotected copper sample (shown in green) exhibits many more peaks and peaks of greater intensity than any other samples at higher frequencies. In Table 1 we also report the power in nm^2 calculated from each of the four sample types. Unlike the RMS roughness calculation, the power calculation suggests the order of surface features is, in order of increasing roughness, (1) as-polished, (2) freshly SAM-protected, (3) two-week SAM-protected, and (4) unprotected. Both Figure 7 and the power calculation in Table 1 demonstrate that the PSD measurement takes into account the lateral spacing between features and clearly shows that the unprotected copper has more high frequency features upon corrosion. Thus, the PSD analysis is a more accurate tool for quantifying these surfaces than the RMS roughness measurement that is typically employed.

© 2000 Springer-Verlag New York, Inc., S1430-4171(00)01350-9, 10.1007/s00897990350a, 510008ba.pdf

Conclusion

We have reported a surface science laboratory exercise suitable for an undergraduate materials science audience in any number of disciplines including chemistry, physics, and engineering. This laboratory provides undergraduate students with an experiment to introduce them to AFM and surface characterization. Students are able to use AFM to observe the real-world problem of metallic surface corrosion, and the concept and application of self-assembled monolayers is demonstrated with this experiment. Students also learn that more than one mathematical technique is often needed to get a complete understanding of images obtained through AFM.

Acknowledgment. The American Chemical Society Petroleum Research Fund Type B (Grant #33989-B5) and the National Science Foundation Research Experiences for Undergraduates (Grant #9731912) provided partial support for this project.

References and Notes

1. Binnig, G.; Quate, C. F.; Gerber, C. *Phys. Rev. Lett.* **1986,** *56,* 930–933.
2. Hansma, P. K.; Elings, V. B.; Marti, O.; Bruker, C. E. *Science* **1988,** *242,* 209–216.
3. Newman, R. C.; Sieradzki, K. *MRS Bulletin* **1999,** *24,* 12–47.
4. Binnig, G.; Rohrer, H.; Gerber, C.; Weibel, E. *Phys. Rev. Lett.* **1983,** *50,* 120–123.
5. Pool, R. *Science* **1990,** *247,* 634–636.
6. Eigler, D. IBM Almaden Research Center STM Image Gallery. http://www.almaden.ibm.com/vis/stm/gallery.htm (accessed Dec 1999).
7. Schaffer, J. P.; Saxena, A.; Andolovich, S. D.; Sanders, T. H.; Warner, S. B. *The Science and Design of Engineering Materials*, 2nd ed.; WCB/McGraw-Hill: Boston, 1999.
8. National Oceanographic and Atmospheric Administration. http://www.nodc.noaa.gov/IMAGES/salinity.gif, (accessed Dec 1999).
9. Bain, C. D.; Troughton, E. B.; Tao, Y.-T.; Evall, J.; Whitesides, G. M.; Nuzzo, R. G. *J. Am. Chem. Soc.* **1989,** *111,* 321–335.
10. Xia, Y.; Kim, E.; Whitesides, G. M. *J. Electrochem. Soc.* **1996,** *143,* 1070–1079.
11. Whitten, D. G.; Kajiyama, T.; Kunitake, T. *MRS Bulletin* **1995,** *20,* 18–58.
12. Schmidt-Rieder, E.; Tong, X. Q.; Farr, J. P. G.; Aindow, M. *Brit. Corrosion J.* **1996,** *31*.
13. Beccaria, A. M.; Padeletti, G.; Montsperilli, G.; Chiaruttini, L. *Surf. Coat. Technol.* **1999,** *111,* 240–246.
14. Cicileo, G. P.; Rosales, B. M.; Varela, F. E.; Vilche, J. R. *Corrosion Sci.* **1998,** *40,* 1915–1925.
15. Hanada, R.; Aramaki, K. *J. Electrochem. Soc.* **1998,** *146,* 1856–1861.
16. Laibinis, P. E.; Whitesides, G. M. *J. Am. Chem. Soc.* **1992,** *114,* 9022–9028.
17. Rohwerder, M.; Stratmann, M. *MRS Bulletin* **1999,** *24,* 43–47.
18. Russ, J. C. *Computer Assisted Microscopy*; Plenum Press: New York, 1990.
19. Russ, J. C. *The Image Processing Handbook,* 2nd ed.; CRC Press: Boca Raton, Fl, 1995.
20. Kiely, J. D.; Bonnell, D. A. *J. Vacuum Sci. and Technol. B* **1997,** *15,* 1483–1493.
21. Spanos, L.; Irene, E. A. *J. Vacuum Sci. and Technol. A* **1994,** *12,* 2646–2652.
22. Kitching, S.; Williams, P. M.; Roberts, C. J.; Davies, M. C.; Tendler, S. J. B. *J. Vacuum Sci. and Technol. B* **1999,** *17,* 273–279.
23. Fang, S. J.; Haplepete, S.; Chen, W.; Helms, C. R.; Edwards, H. *J. Appl. Phys.* **1997,** *82,* 5891–5898.
24. Adamson, A. W.; Gast, A. P. *Physical Chemistry of Surfaces*; 6th ed.; J. Wiley & Sons: New York, 1997.
25. Magnussen, O. M.; Behm, R. J. *MRS Bulletin* **1999,** *24,* 16–23.

© 2000 Springer-Verlag New York, Inc., S1430-4171(00)01350-9, 10.1007/s00897990350a, 510008ba.pdf